Electronic Supplementary Information

Supracolloidal helices from soft Janus particles by tuning particle softness

Qing-Zhi Zou,[†] Zhan-Wei Li,[*,†] Zhong-Yuan Lu,[‡] and Zhao-Yan Sun[*,†]

State Key Laboratory of Polymer Physics and Chemistry, Changchun Institute of Applied Chemistry, Chinese Academy of Sciences, Changchun 130022, China

, and State Key Laboratory of Supramolecular Structure and Materials, Institute of Theoretical Chemistry, Jilin University, Changchun 130023, China

E-mail: zwli@ciac.ac.cn; zysun@ciac.ac.cn

[*]To whom correspondence should be addressed
[†]Changchun Institute of Applied Chemistry
[‡]Jilin University

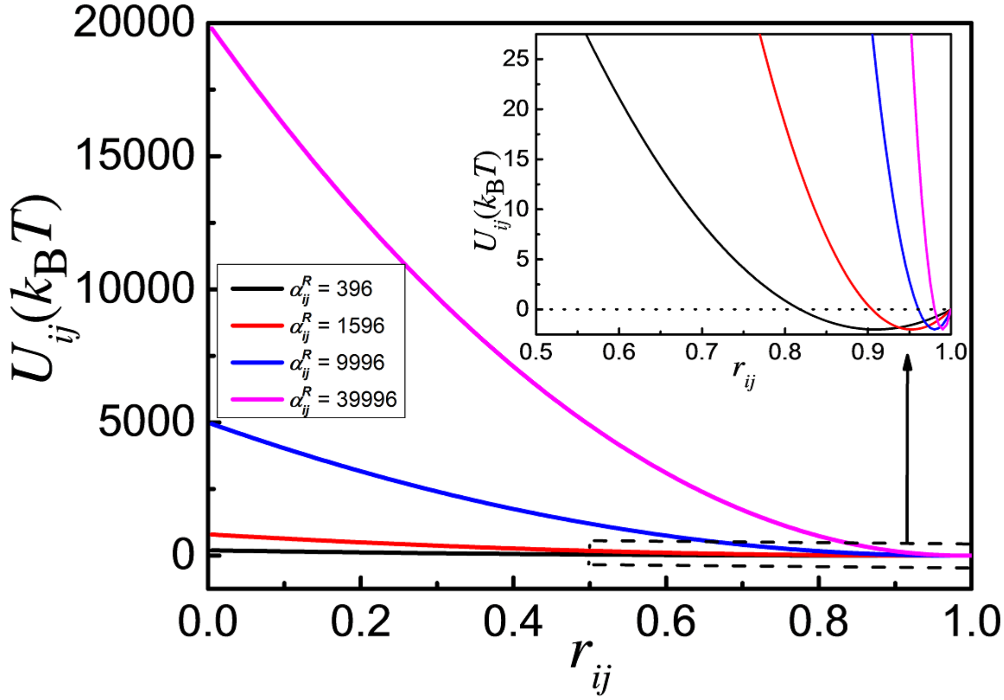

Figure S1: Distance dependence of the anisotropic attractive potential U_{ij} for different α_{ij}^R while keeping the adhesion energy $G = 2.0\ k_B T$ and $\theta_i = \theta_j = 0°$.

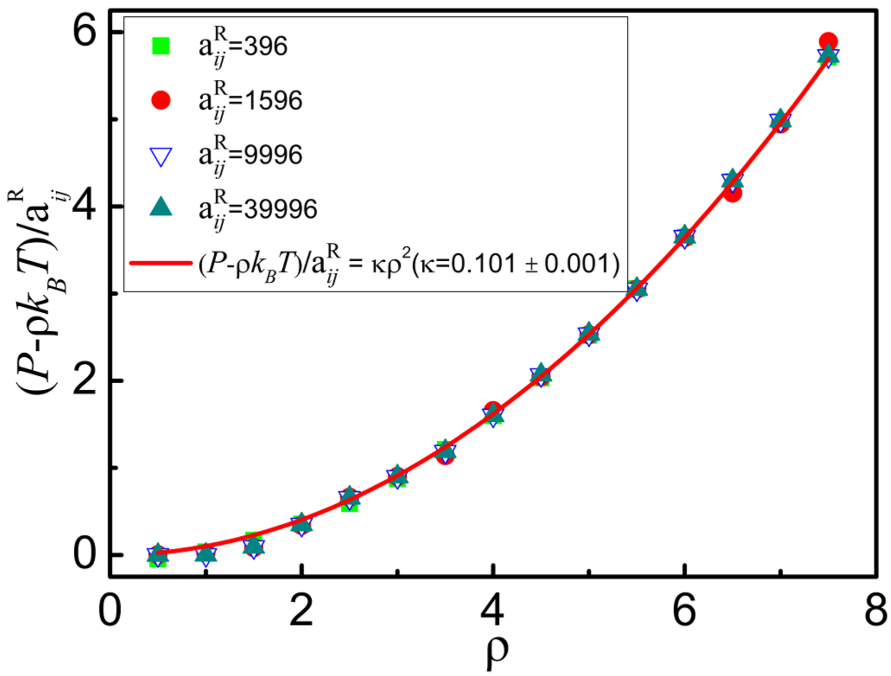

Figure S2: Excess pressure obtained from a series of simulations for the systems with increasing values of $\alpha_{ij}^R = 396$, 1596, 9996, and 39996 in the repulsive potential $U_{ij} = \frac{\alpha_{ij}^R}{2}\left(1 - \frac{r_{ij}}{r_c}\right)^2$, all the relations between the pressure and the number density can be fitted well by a parabola function $p = \rho k_B T + \kappa \alpha_{ij}^R \rho^2$ ($\kappa = 0.101 \pm 0.001$).

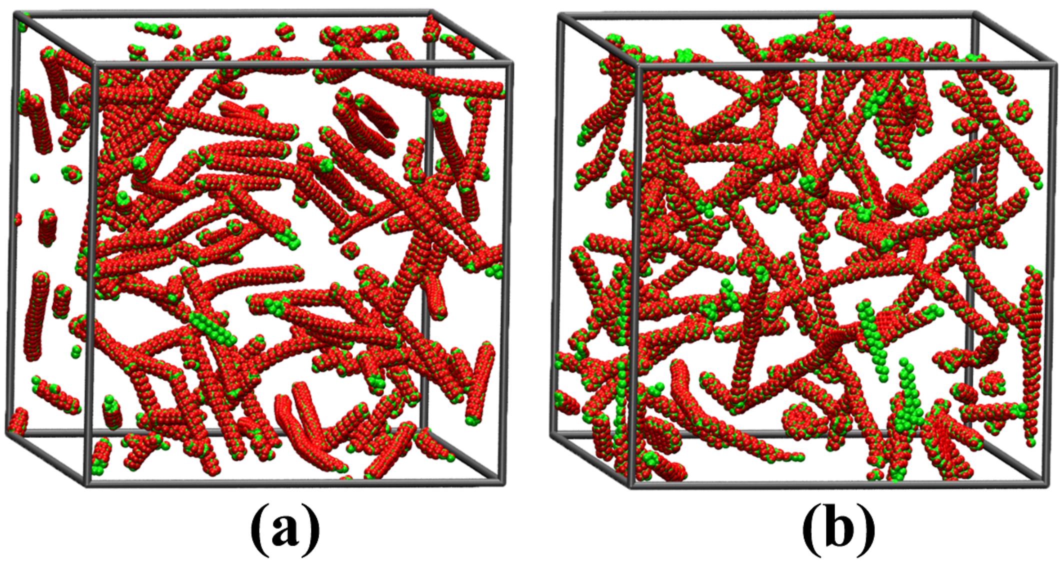

Figure S3: Supercolloidal helices self-assembled from Janus particles for different α_{ij}^{A} and β while keeping $\alpha_{ij}^{R} = 396$, $\nu = 0.5$, and $\phi = 5\%$. (a) Single helices at $\alpha_{ij}^{A} = 308$ ($G \approx 17.00$ k_BT), $\beta = 115°$. (b) Double helices at $\alpha_{ij}^{A} = 242$ ($G \approx 11.50$ k_BT), $\beta = 120°$.

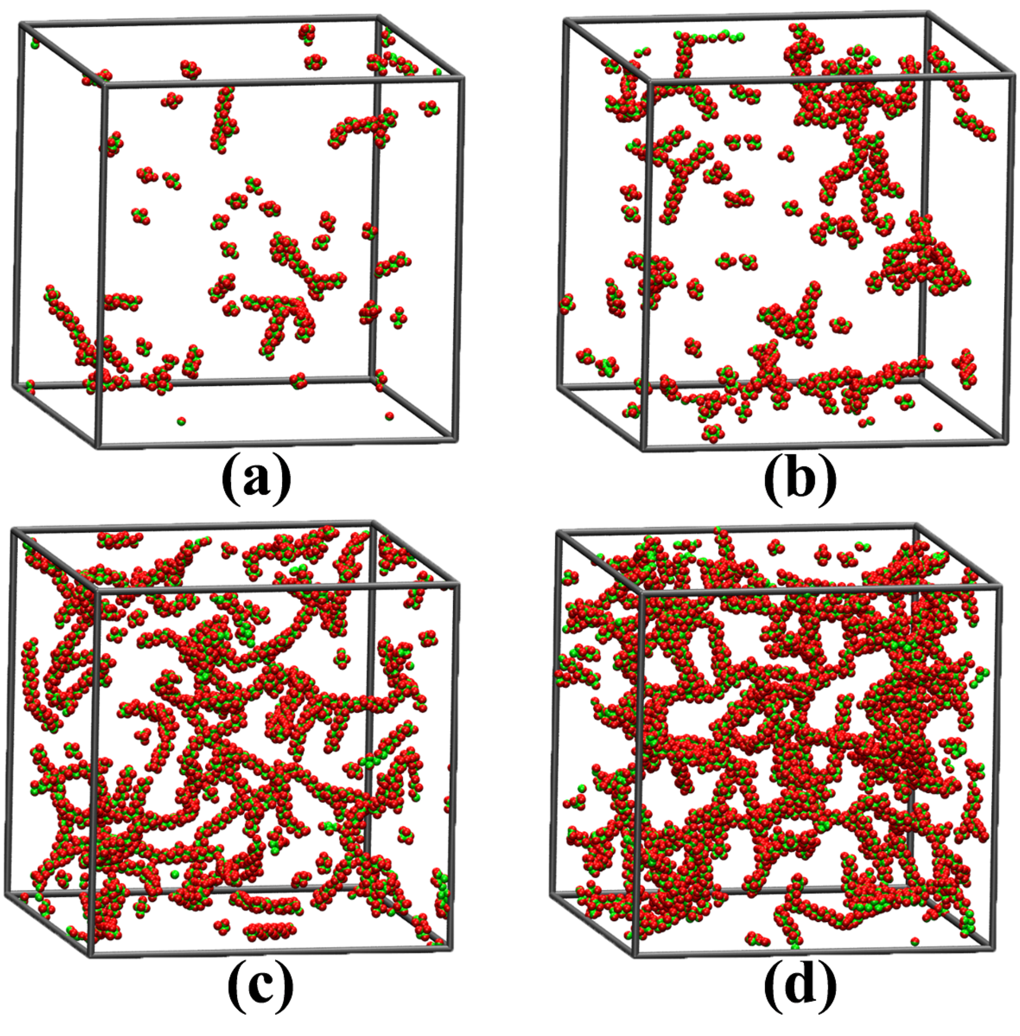

Figure S4: The effect of the concentration of Janus particles ϕ on the formation of Bernal spirals as illustrated in Fig.2d. (a) $\phi = 1\%$. (b) $\phi = 2.5\%$. (c) $\phi = 5\%$. (d) $\phi = 7.5\%$.

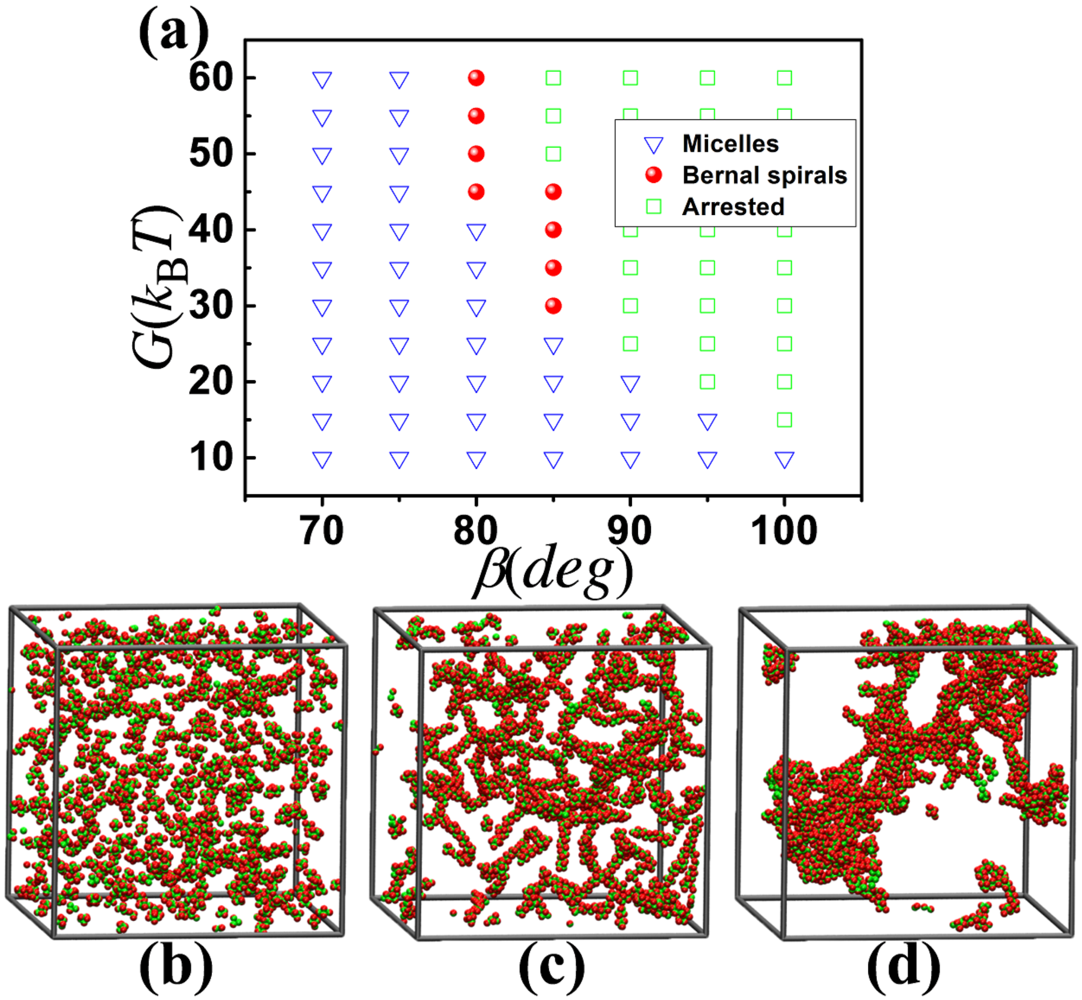

Figure S5: (a) Self-assembly diagram of soft Janus particles in the G-β space at $\alpha_{ij}^{R} = 9996$ ($E = 0.667$ MPa), $\nu = 0.25$, and $\phi = 5\%$. Blue triangles, red spheres, and green squares denote the states with predominantly (b) micellar clusters, (c) Bernal spirals, and (d) the arrested state, respectively.

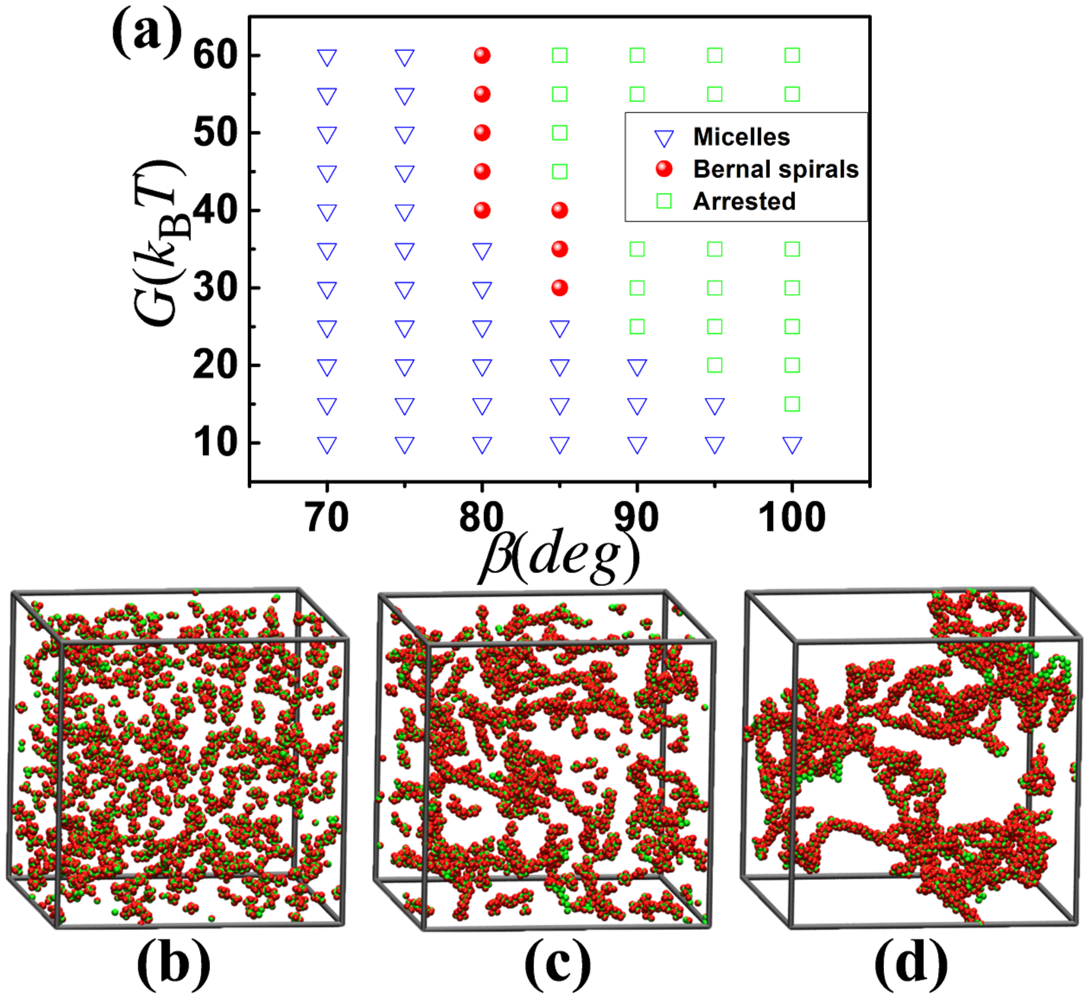

Figure S6: (a) Self-assembly diagram of soft Janus particles in the G-β space at $\alpha_{ij}^R = 1596$ ($E = 0.116$ Mpa), $\nu = 0.25$, and $\phi = 5\%$. Blue triangles, red spheres, and green squares denote the states with predominantly (b) micellar clusters, (c) Bernal spirals, and (d) the arrested state, respectively.

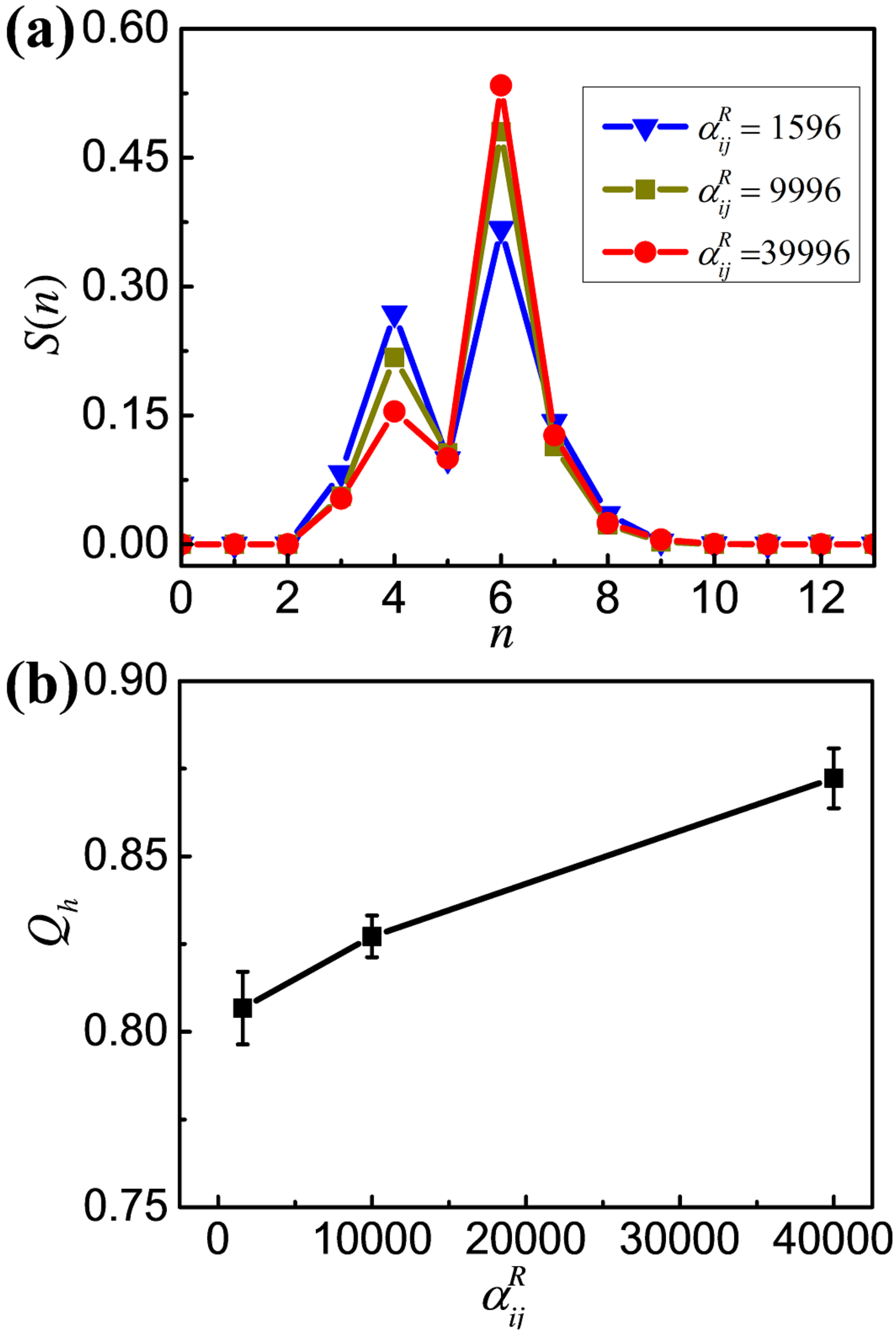

Figure S7: (a) Distribution $S(n)$ of the number of nearest neighbors per Janus particle n, and (b) the helical order parameter Q_h for different α_{ij}^R while keeping adhesion energy $G = 55.00k_BT$, $\beta = 80°$, $\nu = 0.25$ and $\phi = 5\%$.

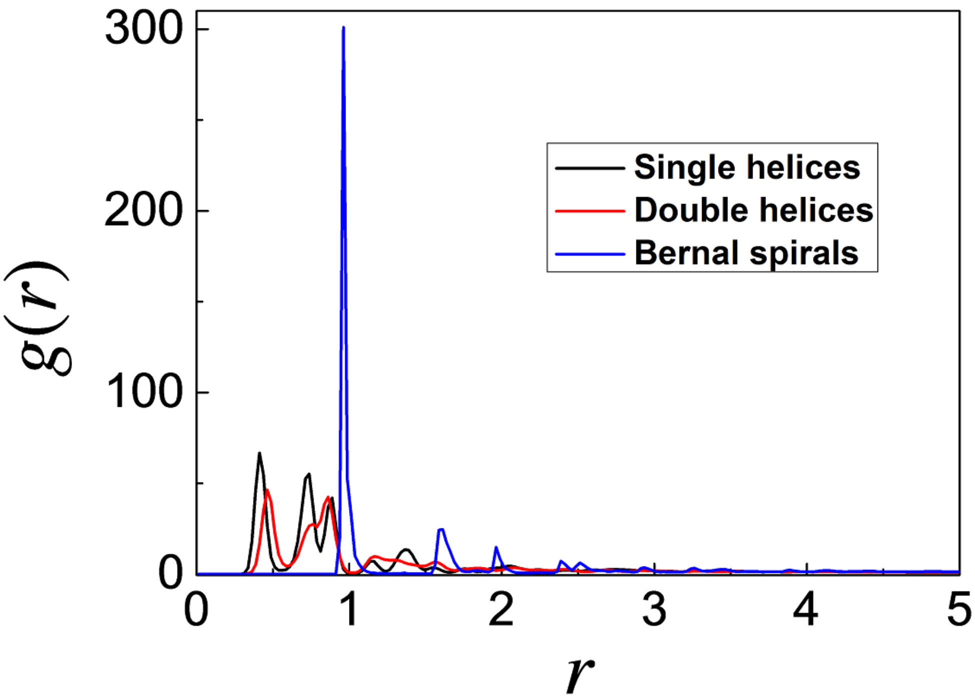

Figure S8: The radial distribution function $g(r)$ for typical self-assembled helical structures in Fig. 3.

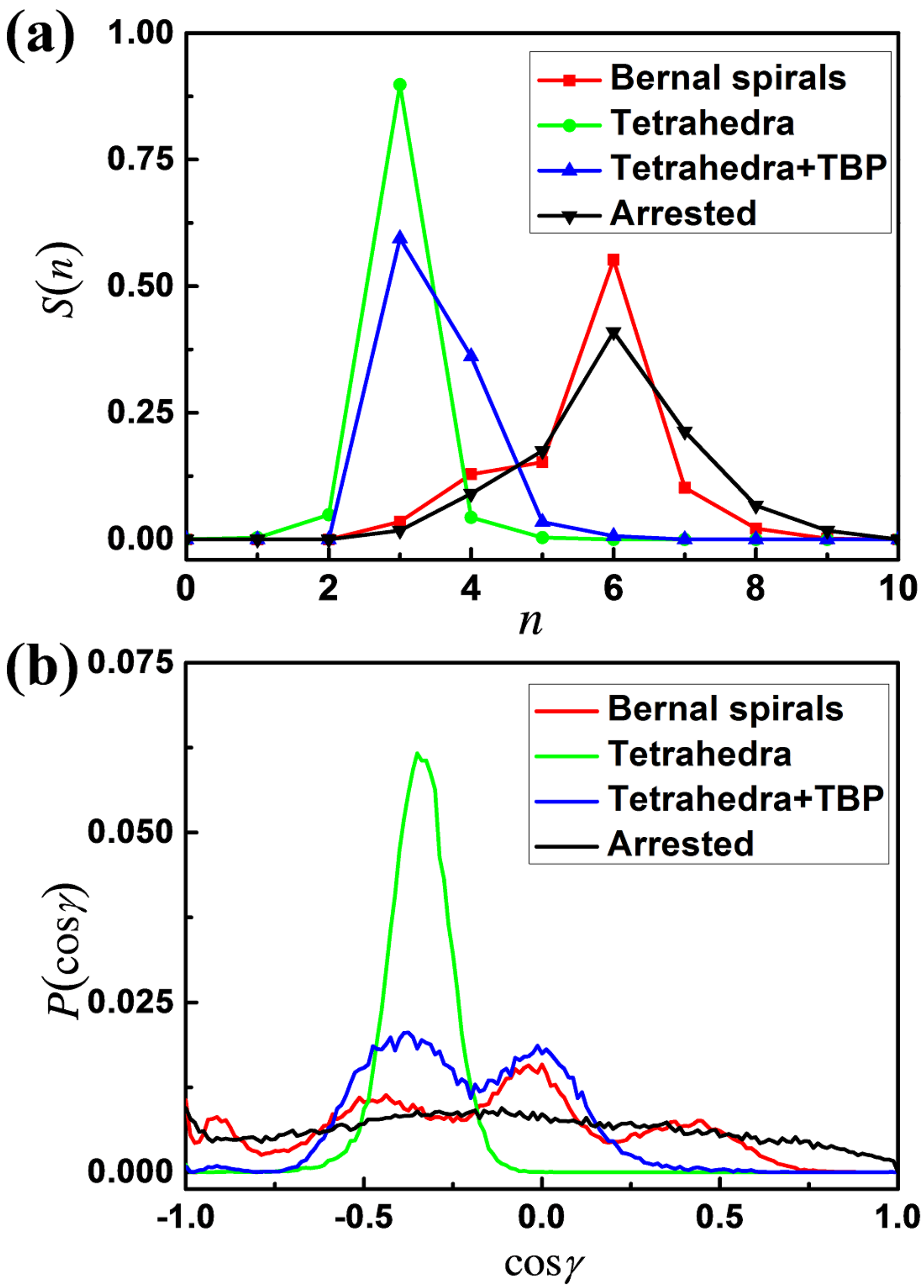

Figure S9: Relative distributions of neighboring particles in typical self-assembled structures in Fig.2. (a) Distribution $S(n)$ of the number of nearest neighbors per Janus particle n. (b) Distribution $P(\cos\gamma)$ of $\cos\gamma = \mathbf{n}_i \cdot \mathbf{n}_j$ for all pairs of contacting Janus particles.

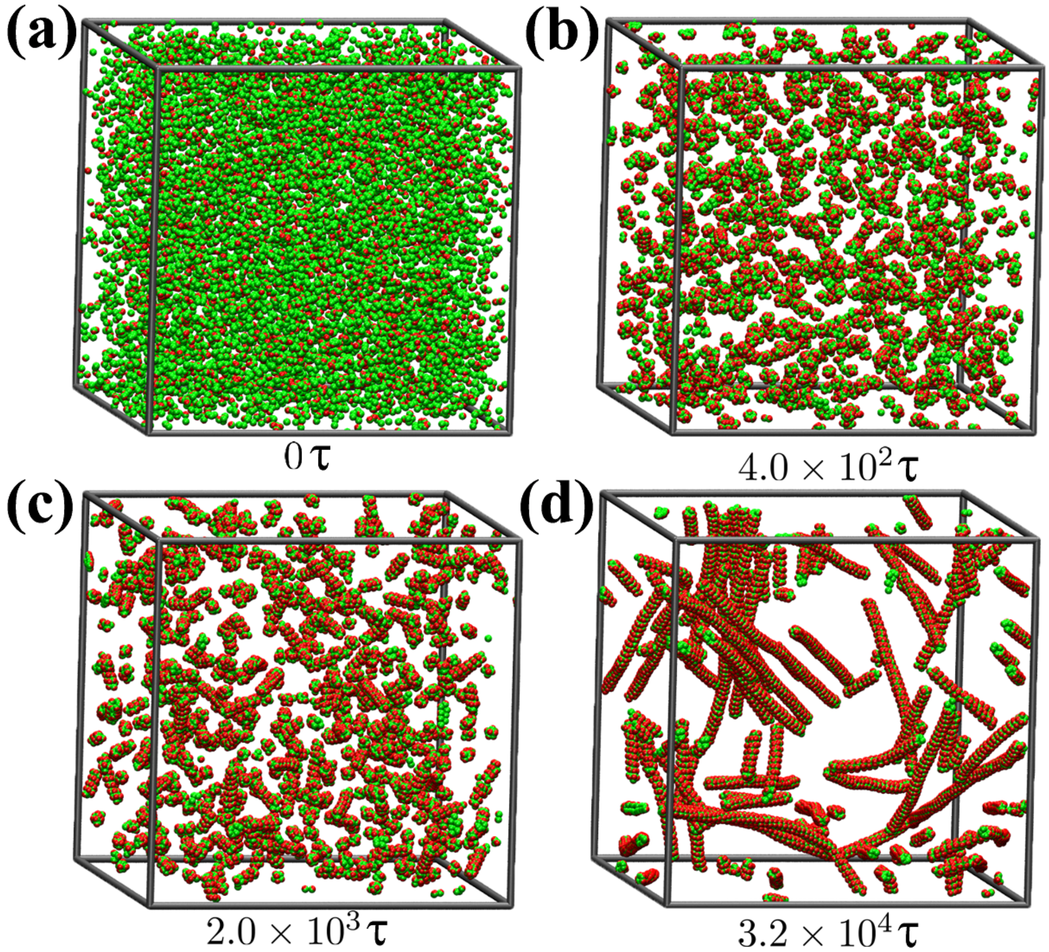

Figure S10: Typical snapshots in the self-assembling process of single helices. (a) 0τ. (b) $4.0 \times 10^2\tau$. (c) $2.0 \times 10^3\tau$. (d) $3.2 \times 10^4\tau$.

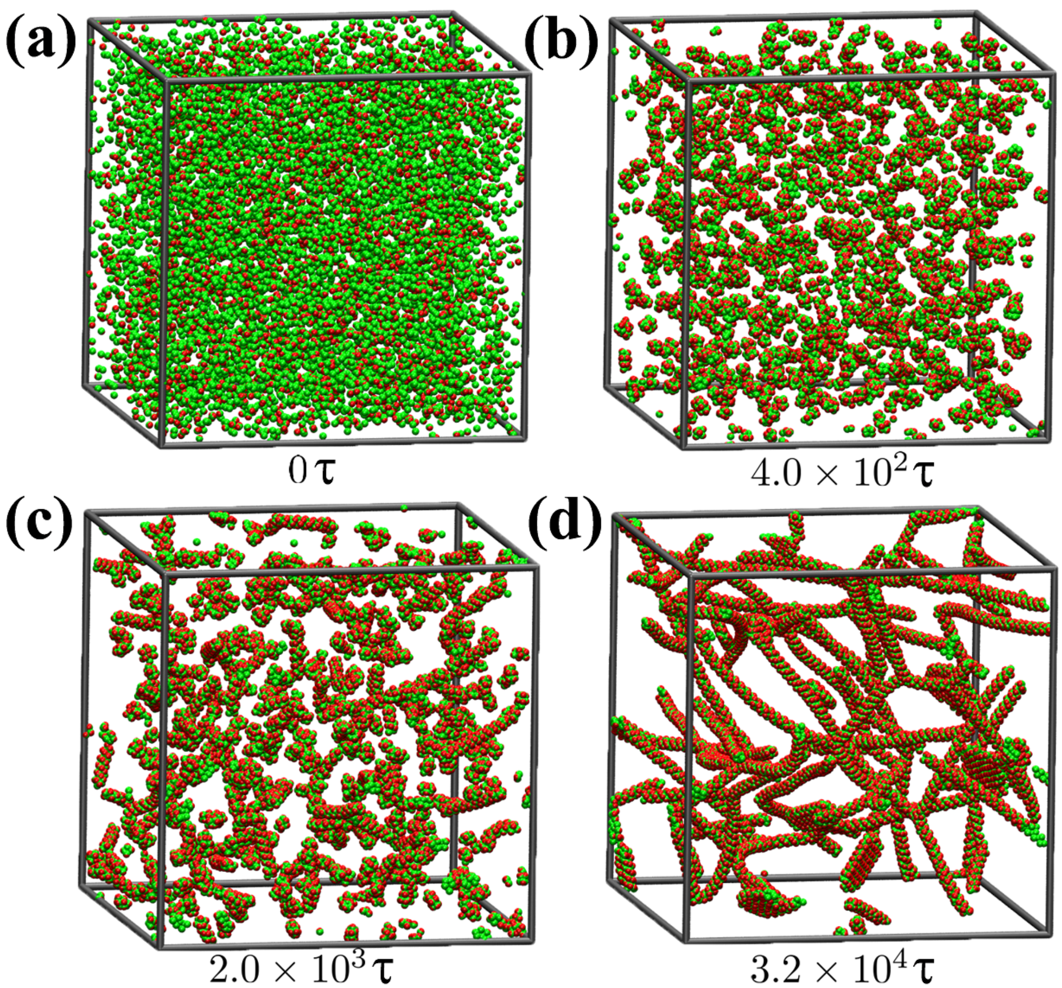

Figure S11: Typical snapshots in the self-assembling process of double helices. (a) 0τ. (b) $4.0 \times 10^2\tau$. (c) $2.0 \times 10^3\tau$. (d) $3.2 \times 10^4\tau$.